# Relationship between trends in land precipitation and tropical SST gradient

## Chul Eddy Chung[1] and V. Ramanathan[1]

[1] Land precipitation trend from 1951 to 2002 shows widespread drying between 10°S to 20°N but the trend from 1977 to 2002 shows partial recovery. Based on general circulation model sensitivity studies, it is suggested that these features are driven largely by the meridional SST gradient trend in the tropics. Our idealized CCM3 experiments substantiate that land precipitation is more sensitive to meridional SST gradient than to an overall tropical warming. Various simulations produced for the IPCC 4th assessment report demonstrate that increasing $CO_2$ increases SST in the entire tropics non-uniformly and increases land precipitation only in certain latitude belts, again pointing to the importance of SST gradient change. Temporally varying aerosols in the IPCC simulations alter meridional SST gradient and land precipitation substantially. Anthropogenic aerosol direct solar forcing without its effects on SST is shown by the CCM3 to have weak but non-negligible influence on land precipitation. **Citation:** Chung, C. E., and V. Ramanathan (2007), Relationship between trends in land precipitation and tropical SST gradient, *Geophys. Res. Lett.*, *34*, L16809, doi:10.1029/2007GL030491.

[2] How much and how exactly do the oceans influence the global atmosphere and hydrological cycle? As far as atmospheric variability, *Charney and Shukla* [1981] demonstrated that tropical variability is largely forced by boundary conditions including SST but not very much so with extratropical variability. Limited to ENSO (El Niño and Southern Oscillation) variability in the Northern Hemisphere (NH) atmosphere, a review paper by *Lau* [1997] showed with GCM (General Circulation Model) experiments that tropical Pacific SSTs alone drive most of NH ENSO variability. Another review study by *Alexander et al.* [2002] clarified the nature of ENSO SST anomalies in the North Pacific. They explained that SST anomalies in the North Pacific are mainly a result of adapting to overlying atmospheric forcing and the influence of these extratropical SSTs on the atmosphere is rather small. Apart from these modeling studies, *Chung et al.* [2002] statistically sought the areas of the Atlantic and Pacific that actively force atmospheric variability. They found that outside of the equatorial Atlantic (10°S–10°N) and outside of the tropical Pacific (30°S–30°N) the oceans passively respond to overlying atmospheric forcing.

[3] The main focus of this study is on decadal to longer time scale trends in land precipitation in association with SST trends. Numerous studies have already pointed to the influence of changes in SST gradients on land precipitation. The Sahelian drought, for example, *Giannini et al.* [2003] attributed to the anomalous warming in the equatorial Atlantic and tropical Indian Oceans, while *Rotstayn and Lohmann* [2002] and *Biasutti and Giannini* [2006] to changes in north–south SST gradient in the Atlantic. *Ramanathan et al.* [2005] and *Chung and Ramanathan* [2006] proposed that the summer-time weakening of the north–south gradient in the tropical Indian Ocean since the 1950s has contributed to the weakening of the summer monsoon in South Asia. *Rotstayn and Lohmann* [2002] furthermore linked the relative N. Atlantic cooling to the aerosol indirect effects. Likewise, *Ramanathan et al.* [2005] attributed the weakening of the Indian Ocean SST gradients to the large dimming by the absorbing aerosols (atmospheric brown clouds) from South and Southeast Asia. In the present study, we expand on these earlier studies, and seek to understand the general relationship between SST and SST gradients and land precipitation on tropical-to-global scales and factor in the effects of aerosols and greenhouse gases.

[4] Figure 1 shows the linear trends of zonal mean SST and land precipitation from observations and numerical simulations. The trends are from 1951 to 2002 (Figures 1a and 1b) and from 1977 to 2002 (Figures 1c and 1d). Note that all of these and the following trends in this study are calculated and displayed in units of change over the whole trend period; i.e., if a 1951–2002 trend is +1.0 K it means 1.0 K increase from 1951 to 2002. For SST observation, Hadley Centre SST [*Rayner et al.*, 2003] is used. Precipitation observation is from Climate Research Unit (CRU) TS 2.1 [*Mitchell and Jones*, 2005]. Time series analysis such as calculating linear trend might be subject to a lot of spurious signals and artifacts in case of precipitation observation analysis, but this problem is minimized as zonal and annual averages are taken. To be sure, we compared the zonal/annual mean time series of CRU product, GPCC (Global Precipitation Climatology Centre) product (B. Rudolf et al., Global precipitation analysis products, 2005, available at http://daac.gsfc.nasa.gov/interdisc/readmes/gpcc.shtml#202), CMAP (CPC Merged Analysis of Precipitation) [*Xie and Arkin*, 1997], GPCP V2 (Global Precipitation Climatology Project Version 2) [*Adler et al.*, 2003], and precipitation analysis by *Hulme et al.* [1998]. Overall features were quite similar. For example, the zonal mean trend from 1979 to 2002 is very similar between the GPCP V2 and CRU. We chose the CRU product for its period availability. In Figure 1, the observation trend uncertainties are displayed with shading.

[5] The observed trends in Figure 1 (red line) provide insight into the sensitivity of land precipitation to SST. During 1951 to 2002, the SST increase between 0° to 30°N

[1]Center for Clouds, Chemistry and Climate, Scripps Institution of Oceanography, La Jolla, California, USA.
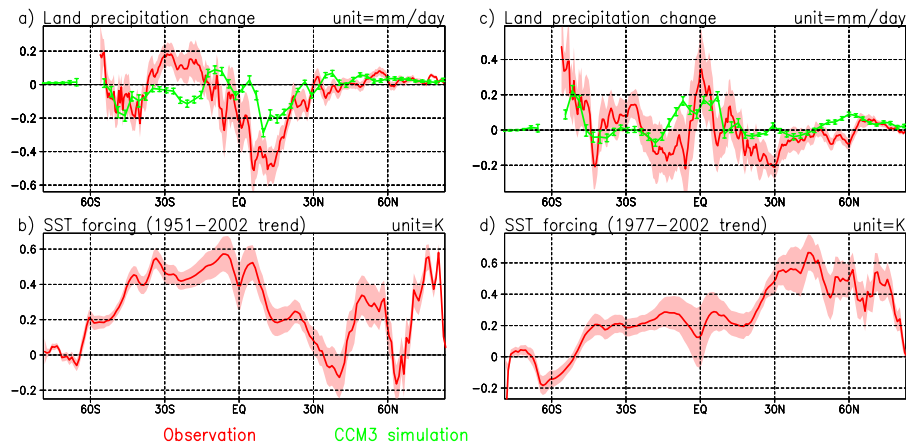
**Figure 1.** Trends in zonal annual mean of land precipitation and SST. (a, b) The 1951–2002 trends. (c, d) The 1977–2002 trends. All of the trends are displayed in units of change over the whole trend period. We used Hadley Centre SST for SST observations and CRU TS 2.1 for land precipitation observations. For land precipitation change simulations, CCM3 was forced by basin-wide-zonal-mean Hadley SST trends. Along with the trends, their ±1.0 S.D. uncertainties are displayed by either shading (observation) or error bar (CCM3). For observation uncertainty, the calculation is against a no real trend scenario, while the CCM3 error calculation is derived from limited ensemble member runs.

was much less than that from $0°$ to $30°$S and the trend in land precipitation is negative between $10°$S to $30°$N. The observed regional precipitation trend during 1951–2002 (not shown) reveals that the drought between $10°$S to $30°$N was widespread across all the continents. The mechanisms whereby meridional SST gradient changes induce remote precipitation changes over land have been suggested before [*Ramanathan et al.*, 2005; *Chung and Ramanathan*, 2006; *Biasutti and Giannini*, 2006]. Basically, deep convection preferably occurs over warmer ocean surface and pressure gradient in the mid and upper troposphere maintains the upper level divergent flow over warmer water. A change in meridional SST gradient alters cross-equatorial pressure gradient and weakens or strengthens meridional moisture flux into land. Where wind direction is mainly zonal, SST gradient change will redistribute zonal moisture flux into land. Furthermore, local changes propagate to other longitudes through the easterly jet.

[6] The SST trend during 1977 to 2002 wiggles without salient gradient features in the tropics, and the precipitation trend is positive in the equatorial region during this period. The relationship between the trends in SST and land precipitation is less obvious for the 1977–2002 period. We conducted a series of numerical experiments with the National Center for Atmospheric Research—Community Climate Model Version-3 (CCM3) [*Kiehl et al.*, 1998] to further explore the relationship.

[7] Figure 1 also shows the CCM3 forced by the observed SST trends (green line). The added observed SST trends in the CCM3 are zonally symmetric with zonal mean taken for each ocean basin. The reason for adding basin symmetric SST is to elucidate the role of meridional SST gradient with respect to land precipitation trend. The CCM3 uses prescribed SSTs. In the control run, the CCM3 (T42/L18 resolution) was run with climatological cycle of SSTs for 85 model years. 85 repetitions is to ensure the statistical significance of the 85 year mean. In one experiment, the basin symmetric trends from 1951–2002 Hadley Centre SST were added to the climatological SSTs.

In another experiment, the 1977–2002 trends were added. Each experiment was run twice with two different initial conditions, and each time for 25 model years with yearly repeating SSTs. After removing the first 2 years, the two of 23 years was averaged to be compared with the 85 year mean in the control run. Our estimates of the uncertainties of the two 23-year run mean are indicated by bar in Figure 1.

[8] The CCM3 simulations correctly capture the drought trend in the northern tropics during 1951 to 2002 (Figure 1a) and its recovery in the equatorial region during 1977 to 2002 (Figure 1c). The CCM3 simulates these precipitation trend features only with the SST forcing that varies meridionally but not zonally. The implication is that land precipitation trend has been driven largely by meridional SST gradient trend. Another implication is the adequacy of the CCM3 in investigating the relationship between meridional SST gradient and land precipitation.

[9] In order to deepen insight into the precipitation/SST relationship, a set of idealized CCM3 experiments were conducted (Figure 2). In each experiment, idealized zonally-symmetric SST anomalies were added to climatological SSTs. The idealized SST forcings are: (1) global weak gradient, (2) sharp gradient in the tropics, (3) sharp gradient in the extratropics, and (4) uniform warming. A uniform and large warming of 1.0 K over the entire global ocean (Figure 2d) leads to rather smaller land precipitation changes than those shown in Figure 1. The sharp sunken SST gradient in the tropics (Figure 2b) produces larger land precipitation changes than any other idealized SST forcing. It is interesting to note that at the bottom of this gradient (around $10°$N; Figure 2b) slightly positive SST anomalies are associated with huge negative precipitation changes, confirming that land precipitation is sensitive to the meridional SST gradient and not much to the SST value itself. In the NH midlatitudes, all the 4 SST forcings produce about 0.1mm/day of precipitation change (equivalently about 5%). The NH midlatitude change pattern by the extratropical sunken gradient (Figure 2c) is quite similar to that by the uniform warming (Figure 2d),
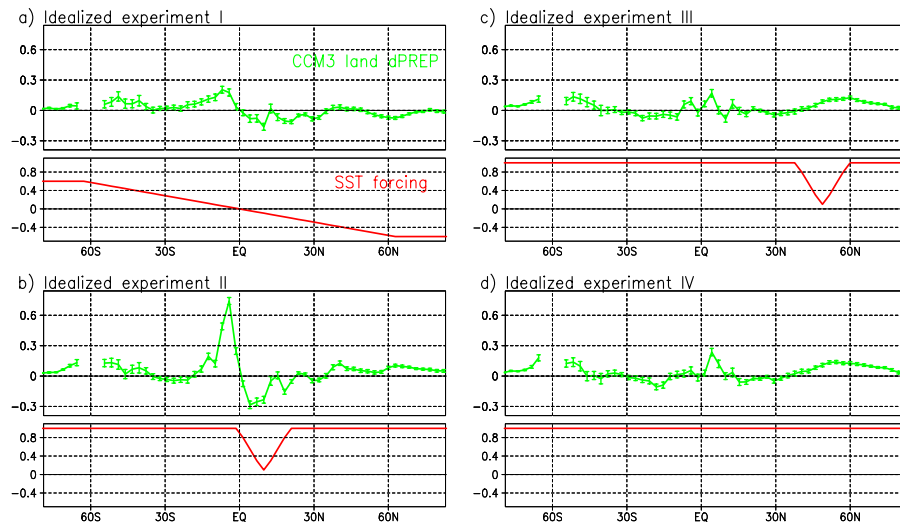
**Figure 2.** Idealized CCM3 experiments. The CCM3 was forced by prescribed SSTs. In each experiment, idealized zonally-symmetric SST anomalies were added to climatological SSTs. Shown in the panels are zonal annual means of added SST anomalies (K) and simulated land precipitation anomalies (mm/day). The ±1.0 S.D. uncertainties are displayed as well for the simulated precipitation.

suggesting that this midlatitude feature came from the tropical SST forcing since these two SST forcings are identical in the tropics (Figures 2c and 2d). Our conclusion from the idealized CCM3 experiments is that the global land precipitation is influenced by tropical SSTs and tropical precipitation is especially vulnerable to meridional SST gradient in the tropics.

[10]  How does tropical SST gradient forcing compare to $CO_2$ and aerosol forcing in influencing land precipitation? It is understood that $CO_2$ influences climate mainly through warming the ocean [*Ramanathan*, 1981]. The mechanism for the effects of aerosols on land precipitation is, to our knowledge, poorly understood. Aerosols, through their so-called direct effects, directly perturb solar radiation (and longwave radiation in the case of dust and sea salt particles) at the surface and in the atmosphere. The aerosol direct forcing leads to a reduction in SST and, in view of regional concentrations of aerosols, to a modification in SST gradient. Aerosol direct forcing also reduces land surface temperature, and enhances solar heating of the atmosphere [*Ramanathan et al.*, 2001]. *Chung et al.* [2005] derived 2001–2003 level global direct anthropogenic aerosol solar radiative forcing by integrating aerosol/cloud observations into a Monte-Carlo radiation model. In their aerosol forcing estimate, the atmosphere heating is very substantial in certain regions due to high regional aerosol concentrations and high percentages of absorbing aerosols such as black carbon (BC) particles. We address the effects of increasing $CO_2$ and anthropogenic aerosols on trends in tropical SST gradient and land precipitation, with the coupled model simulations produced for the Intergovernmental Panel on Climate Change (IPCC) 4th Assessment Report (AR4). We also address the extent to which anthropogenic aerosol direct solar forcing impacts land precipitation without perturbing SST. However, addressing the aerosol indirect effects separately is beyond the scope of this study.

[11]  Figure 3 shows zonal-mean SST change and land precipitation change in the tropics by increasing $CO_2$ only

(Figures 3a and 3b) and by varying greenhouse gases and aerosols together (Figures 3c and 3d) in selected IPCC AR4 model simulations. In the increasing $CO_2$ experiment (Figures 3a and 3b), the $CO_2$ level was increased from its pre-industrial level by 1% per year for 70 years until the level got doubled. In the 20th century experiment (Figures 3c and 3d), greenhouse gases and aerosols were prescribed to vary realistically in time while other climate forcings were held constant. We selected 10 models for the $CO_2$ experiment as summarized in Table 1. The selection was somewhat subjectively done by trying not to pick similar models. Out of these 10 models, we further selected 5 models for the 20th century experiment. These 5 models had fixed natural forcing and land usage while aerosols and greenhouse gases were allowed to vary in time. Shown in Figure 3 are the trends for the last 51 years from the 70 year period in the $CO_2$ experiment (Figures 3a and 3b) and the trends from 1950 to 2000 in the 20th century experiment (Figures 3c and 3d).

[12]  The SST trends in the CO2 experiment are positive in the entire tropics for all the IPCC AR4 simulations (Figure 3a). Most of the models show extra warming features in the equatorial region. The precipitation trends conversely have negative values in certain latitude bands, and in the case of some models (i.e., CSIRO MK3.0 and HadGEM1) the negative pattern is dominating (Figure 3b). The spread among the models is much wider for precipitation trend than for SST trend. The precipitation trend features in all the models appear explainable overall by the trends in SST gradient, in that precipitation trend values are more related to slopes and bell curves in SST trends than to values. We hypothesize that correctly simulating tropical SST gradient trend is one key element in narrowing down the uncertainty for land precipitation trend prediction. Observed 1951–2002 trends are shown by black solid line in Figure 3. It is interesting to note that none of the simulations in the $CO_2$ experiment produces drought at the observed magnitude.
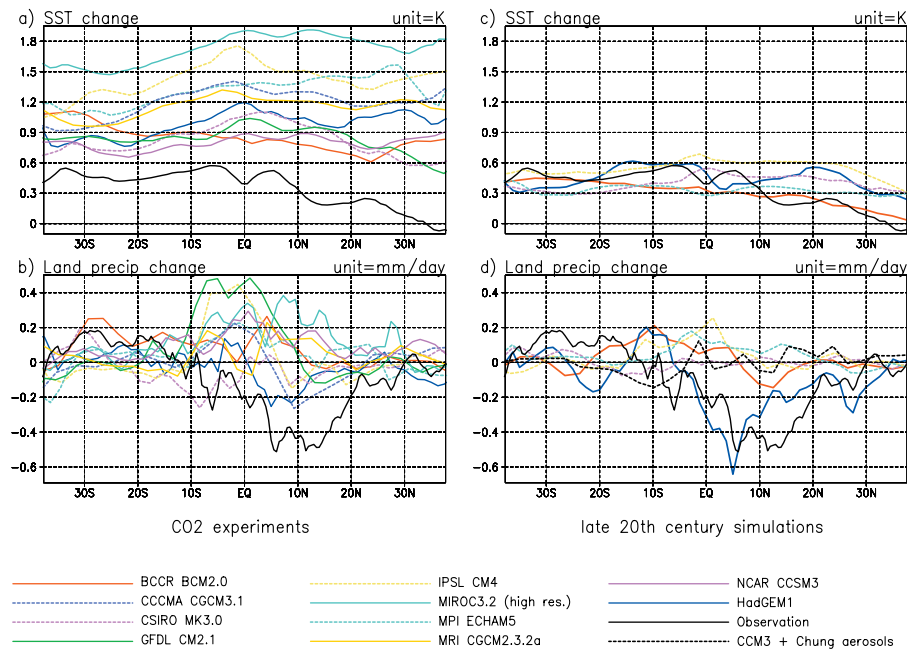
**Figure 3.** Trends of zonal annual means of 10 selected IPCC AR4 coupled models, compared to the observed trend and our CCM3 experiment. (a, b) The trends for the last 51 years in the increasing $CO_2$ IPCC experiments are shown; in these experiments the $CO_2$ level increased by 1% per year for 70 years until the concentration was doubled. (c, d) The trends from 1950 to 2000 in the 20th century IPCC experiments. Figure 3d also includes our CCM3 experiment, where the global anthropogenic aerosol forcing was prescribed while SSTs were held to their climatological values. Superimposed in all the panels are the observed trends from 1951 to 2002. Note from Figures 3c and 3d that the results from BCCR BCM2.0 and HadGEM1 are displayed with extra-thick lines, since only these two models include OC and BC aerosols out of 5 selected IPCC AR4 models.

[13] The SST trends in the 20th century experiment differ considerably from those in the CO2 experiment, in overall warming amplitude and meridional gradient. Much weaker warming amplitudes in the 20th century simulations are believed to be due to exaggerated $CO_2$ increases and the neglect of aerosols in the $CO_2$ experiment. Significant differences in SST gradient, as evident from comparing Figure 3a to Figure 3c, are much greater than the uncertainties in SST gradient trend, and demonstrate that aerosols alter SST gradient substantially. The equatorial extra-warming feature in the $CO_2$ experiment is not strongly noticeable in the 20th century experiment and is absent in the observed trend. In line with differing SST gradient, the precipitation trends in the 20th century experiment

show substantial differences compared to those in the $CO_2$ experiment. Note that simulated drought trend in one model (i.e., HadGEM1) reaches the magnitude in the observed 1951–2002 trend. This model is the only model in Figures 3c and 3d that includes BC and OC aerosols as well as sulfate, and also includes aerosol indirect effects. The spread among the models is even far wider for precipitation trend than for SST trend, compared with that in the $CO_2$ experiment, implying that different aerosol treatments contributed to differences in simulated SST gradient trend.

[14] Figure 3d also includes precipitation change simulated by the CCM3 (black dashed line). In this experiment, the global anthropogenic aerosol direct solar

**Table 1.** IPCC AR4 Coupled Model Simulations Selected for the Present Study[a]

|  | NF | Land | OC/BC | IE | Aerosol Source |
|---|---|---|---|---|---|
| BCCR BCM2.0 | N | N | Y | N | sulfate from *Boucher and Pham* [2002] |
| CCCMA CGCM3.1 | N | N | N | N | sulfate from *Boucher and Pham* [2002] |
| CSIRO MK3.0 | N | N | N | N | sulfate from *Penner et al.* [1994] |
| GFDL CM2.1 | Y | Y | Y | N | from MOZART simulation [*Horowitz et al.*, 2003] |
| IPSL CM4 | N | N | N | Y | sulfate from *Boucher and Pham* [2002] |
| MIROC3.2 (high res.) | Y | Y | Y | Y | SPRINTARS simulation [*Takemura et al.*, 2005] |
| MPI ECHAM5 | N | N | N | Y | sulfate from *Boucher and Pham* [2002] |
| MRI CGCM2.3.2a | Y | N | N | N | sulfate from *Mitchell and Johns* [1997] |
| NCAR CCSM3 | Y | N | Y | N | from MATCH simulation [*Rasch et al.*, 1997] |
| HadGEM1 | N | N | Y | Y | *Roberts and Jones* [2004]; *Woodage et al.* [2003] |

[a]NF: solar activity or volcanic forcing change; land: land use change; OC/BC: OC/BC aerosols included; IE: aerosol indirect effect. The simulations were obtained from https://esg.llnl.gov:8443/index.jsp.

forcing [*Chung et al.*, 2005] was included while SST was held to its climatological cycle. This experiment exposes the effects of aerosols on land precipitation without affecting SST. The result is precipitation change much weaker than the observed, and also weaker than the difference between the $CO_2$ and 20th century experiments. However, the overall precipitation change amplitude is not negligible. These results support the findings of the *Rotstayn and Lohmann* [2002], *Ramanathan et al.* [2005] and *Chung and Ramanathan* [2006] studies that the most effective way for aerosols to impact land precipitation is by perturbing SST gradient.

[15] In summary, land precipitation is more sensitive to trends in tropical SST gradient than to an overall tropical warming. Aerosols, because of their spatial heterogeneity, can potentially have a major impact on land precipitation by perturbing SST gradient in the tropics.

## References

Adler, R. F., et al. (2003), The version 2 Global Precipitation Climatology Project (GPCP) monthly precipitation analysis (1979–present), *J. Hydrometeorol.*, *4*, 1147–1167.

Alexander, M. A., I. Bladé, M. Newman, J. R. Lanzante, N.-C. Lau, and J. D. Scott (2002), The atmospheric bridge: The influence of ENSO teleconnections on air-sea interaction over the global oceans, *J. Clim.*, *15*, 2205–2231.

Biasutti, M., and A. Giannini (2006), Robust Sahel drying in response to late 20th century forcings, *Geophys. Res. Lett.*, *33*, L11706, doi:10.1029/2006GL026067.

Boucher, O., and M. Pham (2002), History of sulfate aerosol radiative forcings, *Geophys. Res. Lett.*, *29*(9), 1308, doi:10.1029/2001GL014048.

Charney, J. G., and J. Shukla (1981), Predictability of monsoons, in *Monsoon Dynamics*, edited by J. Lighthill and R. P. Pearce, pp. 99–109, Cambridge Univ. Press, New York.

Chung, C., and V. Ramanathan (2006), Weakening of N. Indian SST gradients and the monsoon rainfall in India and the Sahel, *J. Clim.*, *19*, 2036–2045.

Chung, C., S. Nigam, and J. Carton (2002), SST-forced surface wind variability in the tropical Atlantic: An empirical model, *J. Geophys. Res.*, *107*(D15), 4244, doi:10.1029/2001JD000324.

Chung, C. E., V. Ramanathan, D. Kim, and I. A. Podgorny (2005), Global anthropogenic aerosol direct forcing derived from satellite and ground-based observations, *J. Geophys. Res.*, *110*, D24207, doi:10.1029/2005JD006356.

Giannini, A., R. Saravanan, and P. Chang (2003), Oceanic forcing of Sahel rainfall on interannual to interdecadal time scales, *Science*, *302*, 1027–1030.

Horowitz, L. W., et al. (2003), A global simulation of tropospheric ozone and related tracers: Description and evaluation of MOZART, version 2, *J. Geophys. Res.*, *108*(D24), 4784, doi:10.1029/2002JD002853.

Hulme, M., T. J. Osborn, and T. C. Johns (1998), Precipitation sensitivity to global warming: Comparison of observations with HadCM2 simulations, *Geophys. Res. Lett.*, *25*, 3379–3382.

Kiehl, J. T., J. J. Hack, G. B. Bonan, B. A. Boville, D. L. Williamson, and P. J. Rasch (1998), The National Center for Atmospheric Research Community Climate Model: CCM3, *J. Clim.*, *11*, 1131–1149.

Lau, N.-C. (1997), Interactions between global SST anomalies and the midlatitude atmospheric circulation, *Bull. Am. Meteorol. Soc.*, *78*, 21–33.

Mitchell, J. F. B., and T. C. Johns (1997), On modification of global warming by sulfate aerosols, *J. Clim.*, *10*, 245–267.

Mitchell, T. D., and P. D. Jones (2005), An improved method of constructing a database of monthly climate observations and associated high-resolution grids, *Int. J. Climatol.*, *25*, 693–712.

Penner, J. E., R. J. Charlson, J. M. Hales, N. S. Laulainen, R. Leifer, T. Novakov, J. Ogren, L. F. Radke, S. E. Schwartz, and L. Travis (1994), Quantifying and minimizing uncertainty of climate forcing by anthropogenic aerosols, *Bull. Am. Meteorol. Soc.*, *75*, 375–400.

Ramanathan, V. (1981), The role of ocean-atmosphere interactions in the $CO_2$ climate problems, *J. Atmos. Sci.*, *38*, 918–930.

Ramanathan, V., et al. (2001), The Indian Ocean Experiment: An integrated analysis of the climate forcing and effects of the Great Indo-Asian Haze, *J. Geophys. Res.*, *106*, 28,371–28,398.

Ramanathan, V., C. Chung, D. Kim, T. Bettge, L. Buja, J. T. Kiehl, W. M. Washington, Q. Fu, D. R. Sikka, and M. Wild (2005), Atmospheric brown clouds: Impacts on South Asian climate and hydrological cycle, *Proc. Natl. Acad. Sci. U. S. A.*, *102*, 5326–5333, doi:10.1073/pnas.0500656102.

Rasch, P. J., N. M. Mahowald, and B. E. Eaton (1997), Representations of transport, convection, and the hydrologic cycle in chemical transport models: Implications for the modeling of short-lived and soluble species, *J. Geophys. Res.*, *102*, 28,127–28,138.

Rayner, N. A., D. E. Parker, E. B. Horton, C. K. Folland, L. V. Alexander, D. P. Rowell, E. C. Kent, and A. Kaplan (2003), Global analyses of sea surface temperature, sea ice, and night marine air temperature since the late nineteenth century, *J. Geophys. Res.*, *108*(D14), 4407, doi:10.1029/2002JD002670.

Roberts, D. L., and A. Jones (2004), Climate sensitivity to black carbon aerosol from fossil fuel combustion, *J. Geophys. Res.*, *109*, D16202, doi:10.1029/2004JD004676.

Rotstayn, L. D., and U. Lohmann (2002), Tropical rainfall trends and the indirect aerosol effect, *J. Clim.*, *15*, 2103–2116.

Takemura, T., T. Nozawa, S. Emori, T. Y. Nakajima, and T. Nakajima (2005), Simulation of climate response to aerosol direct and indirect effects with aerosol transport-radiation model, *J. Geophys. Res.*, *110*, D02202, doi:10.1029/2004JD005029.

Woodage, M., P. Davison, and D. L. Roberts (2003), Aerosol processes, *Unified Model Doc. Pap. 20*, 30 pp., Met Off., Exeter, U. K.

Xie, P., and P. A. Arkin (1997), Global precipitation: A 17-year monthly analysis based on gauge observations, satellite estimates, and numerical model outputs, *Bull. Am. Meteorol. Soc.*, *78*, 2539–2558.

————————————

C. E. Chung and V. Ramanathan, Center for Atmospheric Sciences, Scripps Institution of Oceanography, Mail #0221, 9500 Gilman Drive, La Jolla, CA 92093, USA. (cchung@fiji.ucsd.edu)